Ammonia excretion by the skin of zebrafish (Danio rerio) larvae

Tin-Han Shih, Jiun-Lin Horng, Pung-Pung Hwang and Li-Yih Lin

Am J Physiol Cell Physiol 295:1625-1632, 2008. First published Sep 24, 2008;
doi:10.1152/ajpcell.00255.2008

Am J Physiol Cell Physiol 295: C1625–C1632, 2008.
First published September 24, 2008; doi:10.1152/ajpcell.00255.2008.

Ammonia excretion by the skin of zebrafish (*Danio rerio*) larvae

Tin-Han Shih,[1] Jiun-Lin Horng,[2] Pung-Pung Hwang,[2] and Li-Yih Lin[1]

[1]*Department of Life Science, National Taiwan Normal University, Taipei, Taiwan, Republic of China; and* [2]*Institute of Cellular and Organismic Biology, Academia Sinica, Taipei, Taiwan, Republic of China*

Submitted 14 May 2008; accepted in final form 22 September 2008

Shih TH, Horng JL, Hwang PP, Lin LY. Ammonia excretion by the skin of zebrafish (*Danio rerio*) larvae. *Am J Physiol Cell Physiol* 295: C1625–C1632, 2008. First published September 24, 2008; doi:10.1152/ajpcell.00255.2008.—The mechanism of ammonia excretion in freshwater teleosts is not well understood. In this study, scanning ion-selective electrode technique was applied to measure H^+ and NH_4^+ fluxes in specific cells on the skin of zebrafish larvae. NH_4^+ extrusion was relatively high in H^+ pump-rich cells, which were identified as the H^+-secreting ionocyte in zebrafish. Minor NH_4^+ extrusion was also detected in keratinocytes and other types of ionocytes in larval skin. NH_4^+ extrusion from the skin was tightly linked to acid secretion. Increases in the external pH and buffer concentration (5 mM MOPS) diminished H^+ and NH_4^+ gradients at the larval surface. Moreover, coupled decreases in NH_4^+ and H^+ extrusion were found in larvae treated with an H^+-pump inhibitor (bafilomycin A1) or H^+-pump gene (*atp6v1a*) knockdown. Knockdown of Rhcg1 with morpholino-oligonucleotides also decreased NH_4^+ excretion. This study demonstrates ammonia excretion in epithelial cells of larval skin through an acid-trapping mechanism, and it provides direct evidence for the involvement of the H^+ pump and an Rh glycoprotein (Rhcg1) in ammonia excretion.

H^+-adenosine 5′-triphosphatase; ionocytes; Rhesus glycoprotein; ammonium; knockdown; ion-selective electrode

MOST TELEOSTS EXCRETE AMMONIA (including both NH_3 and NH_4^+) as the primary nitrogenous waste formed mainly from amino acid metabolism (31). The gills are the major site of ammonia elimination in teleosts, but the molecular and cellular mechanisms of ammonia passage through the branchial epithelium are still unclear (5).

The dominant model indicates that branchial ammonia is excreted from freshwater fish mainly down favorable blood-to-water (transbranchial) ammonia gradients (25). Passive NH_3 diffusion is based on evidence that ammonia flow requires a suitable blood-to-water gradient. Ammonia flow is inhibited when the gradient is reduced by high ambient ammonia (1, 29). Wright et al. (33) suggested that maintenance of the transbranchial ammonia gradient relies on acidification of unstirred layers of the apical surface of the branchial epithelium. As it is acidified, this layer creates a microenvironment for a favorable transbranchial NH_3 gradient that facilitates ammonia excretion. This is especially advantageous during exposure to high ammonia (HA), which reverses the normally positive ammonia gradient. Abolishing this layer with HEPES buffer during HA reduced the flux of total ammonia (29). It was also suggested that the H^+ arising from CO_2 hydration traps NH_3 as NH_4^+ as it enters the unstirred layers on the surfaces of gills (29, 33).

In addition to this "acid-trapping" model, early studies proposed the possibility of apical Na^+/NH_4^+ exchange in freshwater teleosts (26). In this model, Na^+ uptake across the apical side of the gill epithelium is linked to NH_4^+ extrusion, which replaces H^+ on the Na^+/H^+ exchanger (NHE). Although, the NHE has been identified in gills of several freshwater species including rainbow trout (*Oncorhynchus mykiss*) (27), tilapia (*Oreochromis mossambicus*) (27), Osorezan dace (*Tribolodon hakonensis*) (8), and zebrafish (*Danio rerio*) (34), the contribution of the apical NHE to ammonia transport has been debated (19, 29).

Recent evidence has shown that the branchial surface might also be acidified by H^+ extruded from an apical vacuolar H^+-ATPase. Accumulating data using pharmacological, physiological, immunocytochemical, and molecular approaches have demonstrated the role of V-type H^+-ATPase in the apical Na^+ uptake mechanism of freshwater teleosts (3, 11). Recently, Nawata et al. (19) examined the mRNA expression of Rhesus (Rh) protein (a putative ammonia transporter/channel), and H^+-ATPase with a real-time PCR in rainbow trout exposed to HA. They found that Rhcg2, Rhbg, and H^+-ATPase (the B-subunit) mRNA expressions were upregulated in pavement cell fractions during HA, and they suggested the contribution of Rh proteins and H^+-ATPase to ammonia transport across gill epithelium. However, direct evidence by a loss-of-function or gain-of-function study has not yet reported. Several isoforms of the Rh glycoprotein (Rhag, Rhbg, Rhcg1, and Rhcg2) have been identified in the gill epithelium of pufferfish (*Takifugu rubripes*) (18), killifish (*Kryptolebias marmoratus*) (10), and zebrafish (17); however, their exact functions are still unclear.

The zebrafish (*D. rerio*) has been used as a good model for studying ion and acid-base regulation in freshwater teleosts (11). Lin et al. (16) identified two subtypes of ionocytes, Na^+ pump-rich cells and H^+ pump-rich (HR) cells in zebrafish larva, by molecular and electrophysiological approaches. Knockdown of H^+-ATPase translation with specific morpholino oligonucleotides (MOs) (9) and bafilomycin inhibition (16) demonstrated that H^+-ATPase contributes to acid secretion in the skin of zebrafish larvae. Recently, Nakada et al. (17) reported that Rhcg1 was located in the apical membrane of HR cells in zebrafish. Therefore, we hypothesized that the HR cells are the main locations for ammonia excretion in zebrafish. We attempted to measure NH_4^+ excretion in specific skin cells with scanning ion-selective electrode technique (SIET), and we provide direct evidence for the contributions of H^+-ATPase and Rhcg1 in ammonia excretion.

MATERIALS AND METHODS

Zebrafish and artificial water. Mature zebrafish (AB strain) were reared in circulating tap water at 28°C with a photoperiod of 12-h

Address for reprint requests and other correspondence: L. Y. Lin, Dept. of Life Science, National Taiwan Normal Univ., Taipei 116, Taiwan, ROC (e-mail: linly@ntnu.edu.tw).

The costs of publication of this article were defrayed in part by the payment of page charges. The article must therefore be hereby marked "*advertisement*" in accordance with 18 U.S.C. Section 1734 solely to indicate this fact.

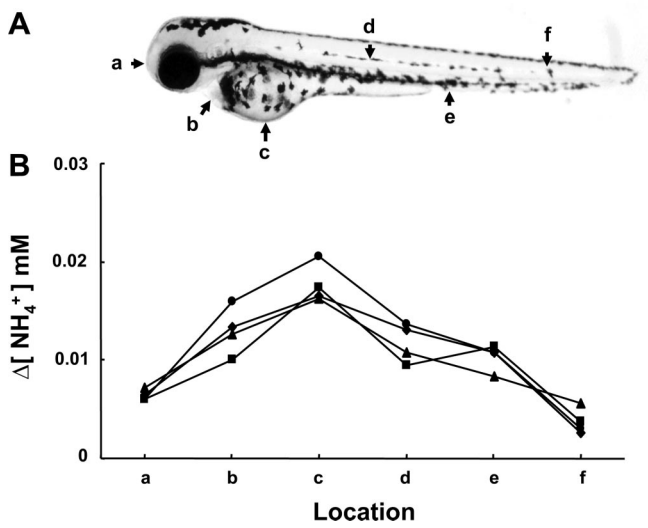

Fig. 1. Ammonium gradient ($\Delta[NH_4^+]$) at the surface of a zebrafish larva. *A*: the 6 spots measured with ion-selective electrode technique (SIET): snout (*a*), pericardial cavity (*b*), yolk sac (*c*), trunk (*d*), cloaca (*e*), and tail (*f*). *B*: $\Delta[NH_4^+]$ measured at 6 spots of 4 individuals.

light/12-h dark. Fertilized eggs were incubated in normal water (NW), which contained (in mM) 0.5 NaCl, 0.2 $MgSO_4$, 0.2 $CaSO_4$, 0.005 KH_2PO_4, and 0.08 K_2HPO_4 (pH 7.0). Fish exposed to HA were acclimated to NW to which NH_4Cl was added. The experimental protocols were approved (no. 95013) by the National Taiwan Normal University Animal Care and Utilization Committee.

Scanning ion-selective electrode technique. To measure NH_4^+ and H^+ activities and fluxes at the surface of zebrafish larvae, NH_4^+- and H^+-selective microelectrodes were constructed. Glass capillary tubes (no. TW 150-4, World Precision Instruments, Sarasota, FL) were pulled on a Sutter P-97 Flaming Brown pipette puller (Sutter Instruments, San Rafael, CA) into micropipettes with tip diameters of 3–4 μm. These glass micropipettes were baked at 120°C overnight and then vapor-silanized with dimethyl chlorosilane (Fluka, Buchs, Switzerland) for 30 min. Before use, the micropipettes were backfilled with 1 cm of a column of 100 mM NH_4Cl or KH_2PO_4 to respectively create an NH_4^+ or H^+ microelectrode. Then the micropipettes were frontloaded with a 20- to 30-μm column of liquid ion exchanger cocktail (NH_4^+ ionophore I *cocktail A* or H^+ ionophore I *cocktail B*; Fluka). The details of the system were described in a previous report (16). The Nernstian property of each microelectrode was measured by placing the microelectrode in a series of standard solutions (0.1, 1, and 10 mM NH_4Cl; pH 6, 7, and 8). By plotting the voltage output of the probe against the log NH_4^+ and H^+ concentrations, a linear regression yielded a Nernstian slope of 57.8 ± 0.6 (n = 10) for NH_4^+ and 57.5 ± 2.5 (n = 10) for H^+.

Measurement of surface NH_4^+ and H^+ gradients. SIET was performed at room temperature (26–28°C) in a small plastic recording chamber filled with 1 ml "recording medium" that contained NW, 300 μM MOPS buffer (Sigma, St. Louis, MO), and 0.1 mg/l ethyl 3-aminobenzoate (Tricaine, Sigma; pH 7.0). The selectivity coefficients of the Fluka NH_4^+ ionophore I (*cocktail A*) is only four times more selective for NH_4^+ than for K^+. Therefore "K^+-free recording medium" (in which KH_2PO_4 and K_2HPO_4 were replaced by NaH_2PO_4 and Na_2HPO_4) was used to probe for NH_4^+. Before the measurement, an anesthetized embryo was positioned in the center of the chamber with its lateral side contacting the base of the chamber. To record the NH_4^+ or H^+ activities at the surface of a larva, the microelectrode was moved to the target position 10–20 μm away from the skin. After recording a target point, the microelectrode was then moved away (~10 mm) to record the background. In this study, $\Delta[NH_4^+]$ and

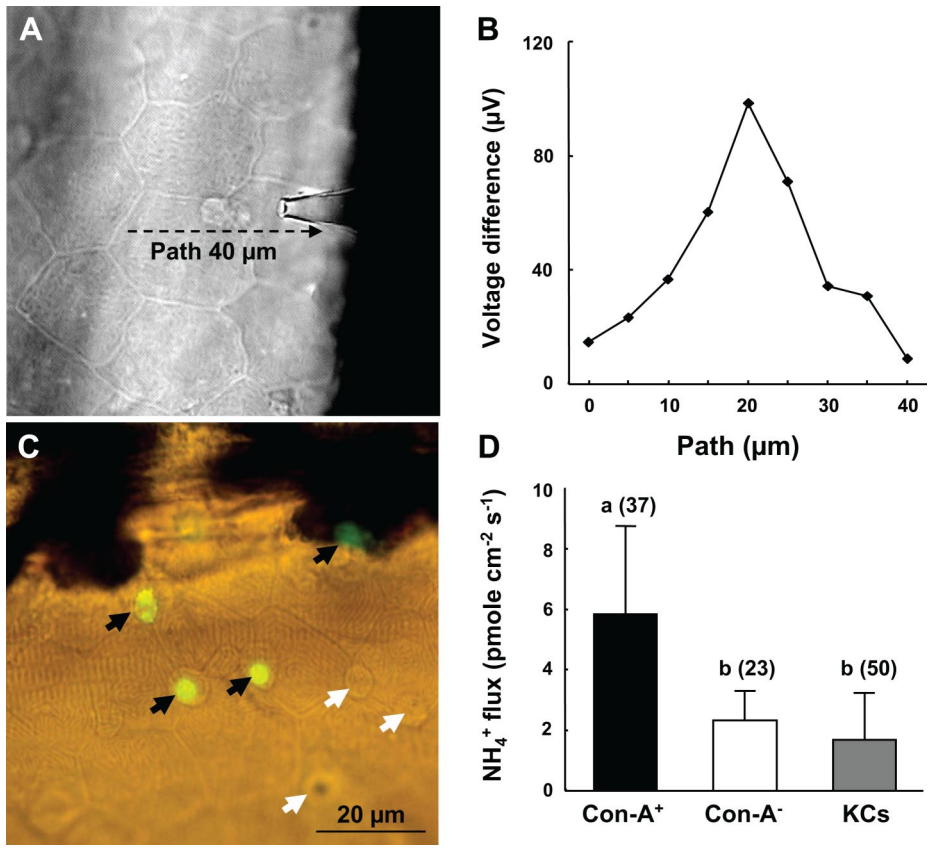

Fig. 2. NH_4^+ fluxes at H^+ pump-rich cells (HRCs) [concanavalin A^+ (Con-A^+)], keratinocytes (KCs), and other ionocytes (Con-A^-). *A*: under a microscope, apical membranes of ionocytes were identified, and a "line scan" was made by probing at a series of locations along a line (arrow) across the surface of the ionocytes and adjacent keratinocytes. *B*: measured NH_4^+ fluxes of the line scan over the surface of an HRC are shown. *C*: the measured ionocytes were further discriminated into a Con-A^+ (HRC) or Con-A^- (non-HRC) group by fluorescent Con-A labeling. *D*: NH_4^+ effluxes (means ± SD, n = 37, 23, and 50, respectively) from different types of cells were compared. Different letters indicate a significant difference (one-way ANOVA, $P < 0.05$).

$\Delta[H^+]$ were respectively used to represent the measured NH_4^+ and H^+ gradients between the point of interest (skin surface) and background.

Measurement of NH_4^+ flux in ionocytes and keratinocytes. The anesthetized larva was laid laterally in the chamber for SIET measurements. Under a differential interference contrast (DIC) microscope, the apical membrane of ionocytes could be identified in its skin. To record the local NH_4^+ flux at specific cell surface sites, the microelectrode was moved to a position 2–3 μm above the surface of interest. In addition to "single-spot" recordings, a "line scan" was made by probing a series of spots along a line (9 spots along 40 μm) across the surface of ionocytes and adjacent keratinocytes. At every spot, the voltage difference in microvolts was measured by probing orthogonally to the surface at 10-μm intervals. The calculation of NH_4^+ flux was shown in previous reports (4, 6). Briefly, voltage gradients obtained from the ASET software were converted into concentration (activity) gradient using the following equation:

$$\Delta C = C_b \times 10^{(\Delta V/S)} - C_b, \quad (1)$$

where ΔC is the concentration gradient between the two points measured in $\mu mol \cdot l^{-1} \cdot cm^{-3}$; C_b is the background ion concentration, calculated as the average of the concentration at each point measured in μmol/l; ΔV is the voltage gradient obtained from ASET in μV; and S is the Nernst slope of the electrode. The concentration gradient was subsequently converted into (extracellular) ion flux using Fick's law of diffusion in the following equation:

$$J = D(\Delta C)/\Delta X \quad (2)$$

where J is the net flux of the ion in $pmol \cdot cm^{-2} \cdot s^{-1}$, D is the diffusion coefficient of the ion (2.09×10^{-5} cm^2/s for NH_4^+ and 9.4×10^{-5} cm^2/s for H^+), ΔC is the concentration gradient in $pmol/cm^3$, and ΔX is the distance between the two points measured in centimeters.

Concanavalin A labeling. Concanavalin A (Con-A), a kind of lectin, was found to bind with the apical membrane of HR cells and was used as a vital marker for HR cells (16). Live larvae were incubated in NW containing 0.5 mg/ml Alexa 488-conjugated Con-A (Molecular Probes, Eugene, OR) for 10 min. After staining, the larvae were washed with NW for 3 min.

Treatment with amiloride, 5-ethylisopropyl amiloride, and bafilomycin A1. The amiloride or 5-ethylisopropyl amiloride (EIPA; Sigma) stock solutions were prepared by dissolving amiloride or EIPA in dimethyl sulfoxide (DMSO, Sigma). A final concentration of 0.1 mM or 1 mM was applied to the larvae for 10 min. After treatment, the larvae were immediately measured with SIET. The bafilomycin A1 (Sigma) stock solution was dissolved in DMSO and then added to the media to a final concentration of 10 μM. The larvae were incubated in 10 μM bafilomycin A1 for 1 h and then measured with SIET. Effect of DMSO has been tested in a preliminary experiment. DMSO did not affect H^+ or NH_4^+ gradient, thus we used NW as control in the inhibitor experiments.

Morpholino design and microinjection. MOs were obtained from Gene Tools (Philomath, OR). The detailed method was previously reported (9). The MOs against H^+-ATPase (*atp6v1a*) and Rhcg 1 were *atp6v1a* (5′-ATCCATCTTGTGTGTTAGAAAACTG-3′) and *rhcg1* (5′-CAGTTGCCCATGTCTACAGCTTGAG-3′), which covers the start codon of Rhcg1. A standard control MO (5′-CCTCTTACCTCAGTTACAATTTATA-3′) was used as the control. The standard control oligo provided by Gene Tools has no target and no significant biological activity. The MO solution was prepared with sterile water and contained 0.1% phenol red as a visualizing indicator. The MO at 8 ng was microinjected into the embryo at the 1- to 4-cell stage with an IM-300 microinjector system (Narishigi Scientific Instrument Laboratory, Tokyo, Japan). In the preliminary test and our previous study (9), embryos injected with 8 ng of control MO showed no significant difference in survival rate, morphology, or H^+ or NH_4^+ secretion (measured with SIET) compared with wild-type embryos, indicating that an injection of 8 ng control MO caused little or no specific effect.

Immunohistochemistry. Zebrafish larvae were anesthetized on ice and fixed with 4% paraformaldehyde in 0.1 M phosphate buffer (pH 7.4) for 1 h at 4°C. After being rinsed with PBS, the larvae were postfixed and permeabilized with 90% ethanol at −20°C for 10 min. After being washed with PBS, samples were incubated with 3% bovine serum albumin and 5% normal goat serum for 30 min to block nonspecific binding. The larvae were then incubated overnight at 4°C with polyclonal antibody against zebrafish Rhcg1 (diluted 1:1,000 with PBS). The antibody was provided by Dr. S. Hirose (17). After being rinsed with PBS for 20 min, the larvae were further incubated in goat anti-rabbit IgG conjugated with FITC (diluted 1:1,000; Jackson Immunoresearch Laboratories, West Grove, PA), for 2 h at room temperature (26–28°C).

RESULTS

NH_4^+ gradients at the skin of zebrafish larvae. Surface NH_4^+ gradients of 5-day postfertilization (dpf) zebrafish larvae were measured with SIET to determine the NH_3/NH_4^+ excretion by larval skin. Six spots on the surface of a larva were chosen for measurement: snout, pericardial cavity, yolk sac, trunk, cloaca, and tail (Fig. 1, *Aa–Af*). $\Delta[NH_4^+]$ at the six spots was deter-

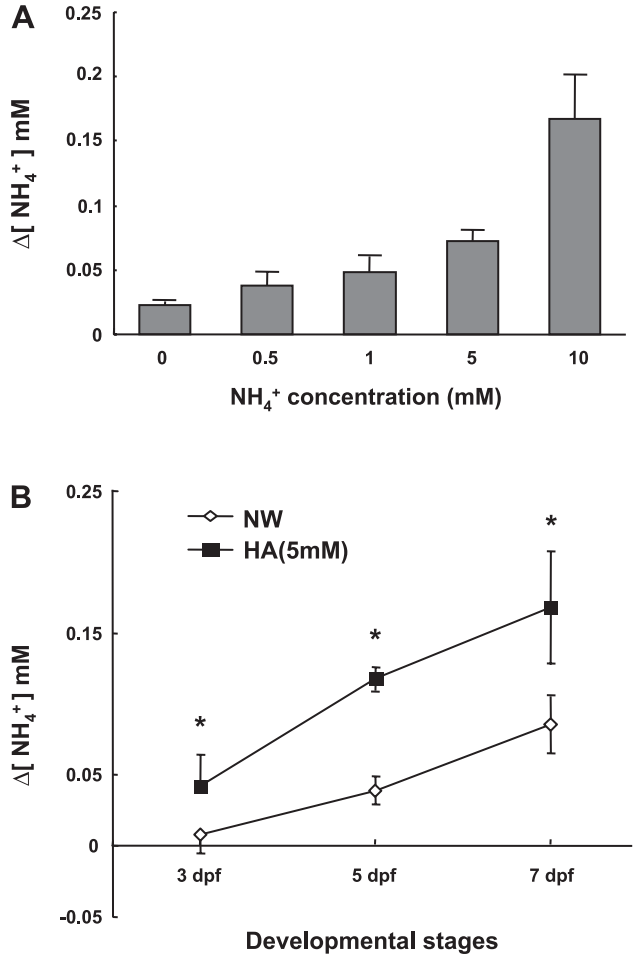

Fig. 3. *A*: $\Delta[NH_4^+]$ at the yolk sac surface of larvae acclimated to various concentrations (0–10 mM) of NH_4Cl. *B*: developmental change in $\Delta[NH_4^+]$ at the yolk sac surface of larvae acclimated to normal water (NW) or high ammonium (HA; 5 mM). In 7 days postfertilization (dpf) larvae, gills were measured because of the disappearance of the yolk sac. Data are presented as means ± SD ($n = 10$). *Significant difference between NW and HA larvae at the same stage (Student's t-test, $P < 0.05$).

mined by calculating the difference between the target spot and background (~10 mm away from the larva). Figure 1*B* shows $\Delta[NH_4^+]$ values measured at the six spots from four individuals. $\Delta[NH_4^+]$ at the yolk sac was higher than at the other locations, indicating that NH_4^+ was highly secreted in the yolk sac area. When the microelectrode was moved step by step away from the yolk sac surface, $[NH_4^+]$ gradually declined with distance (data not shown).

Extracellular NH_4^+ flux in specific cell types on larval skin. Using the NH_4^+-selective microelectrode, NH_4^+ flux at specific cells was measured by probing $\Delta[NH_4^+]$ at 10-μm intervals. Under a microscope, ionocytes and keratinocytes can easily be identified by their morphology (oval and polygonal, respectively; Fig. 2*A*). The measured ionocytes were located mainly in the border between the yolk-extension and trunk of larvae. Figure 2*B* shows a serial probing (line scan) over the surface of an ionocyte, which was further identified as an H^+ pump-rich cell (HRC) by fluorescent Con-A, which is a specific and vital marker for HRCs (16; Fig. 2*C*). SIET detected weaker outward flux of NH_4^+ in keratinocytes, but this gradually increased when probing toward the apical surface of an HRC (Fig. 2*B*). In contrast, no surge in the signal was found when probing over the surface of Con-A-negative cells (other types of ionocytes). Figure 2*D* shows a comparison of NH_4^+ flux in HRCs (Con-A^+), other ionocytes (Con-A^-), and keratinocytes (KCs). The flux from HRCs was about threefold higher than that from other cell types.

NH_4^+ gradients in larvae acclimated to HA. Since the yolk sac area dominates NH_4^+ secretion in larvae, this area was chosen to measure NH_4^+ gradients. $\Delta[NH_4^+]$ was measured in 5-dpf larvae that had been preacclimated to various concentrations of NH_4^+ (0, 0.5, 5, and 10 mM) for 5 days (Fig. 3*A*). During acclimation, no significant increase in mortality was found even in 10 mM HA, indicating that zebrafish can tolerate HA. When the larvae in the recording medium (containing 0.1 mM NH_4Cl) were measured, NH_4^+ gradients showed a dose-dependent increase with the amount of treated $[NH_4^+]$ (Fig. 3*A*). Moreover, the NH_4^+ gradients of larvae also increased

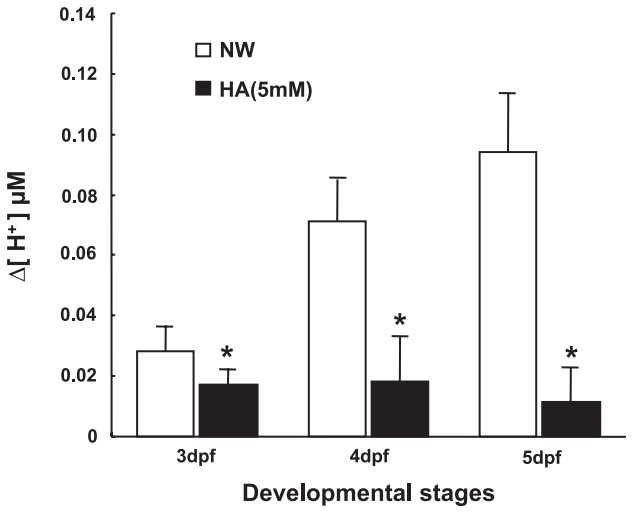

Fig. 4. H^+ gradient ($\Delta[H^+]$) at the yolk sac surface of larvae acclimated to NW or HA (5 mM). Three developmental stages (3, 4, and 5 dpf) are shown. Data are presented as means ± SD ($n = 10$). *Significant difference between NW and HA larvae at the same stage (Student's *t*-test, $P < 0.05$).

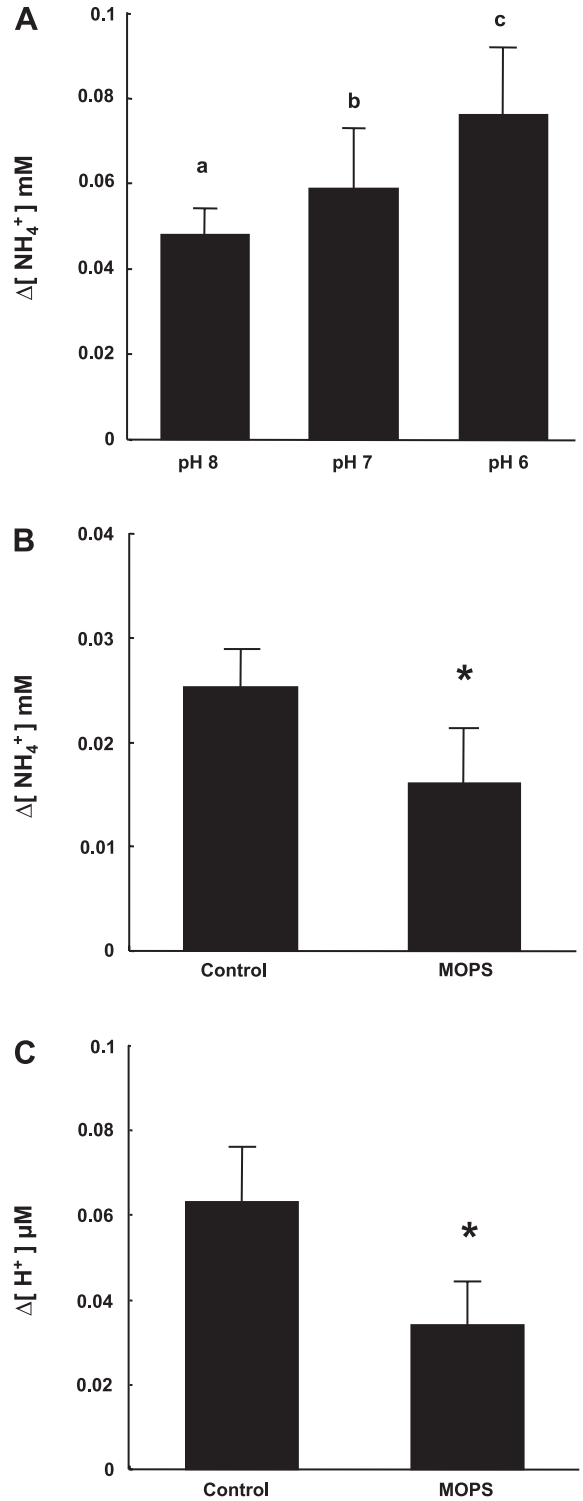

Fig. 5. Effects of external pH (*A*) and MOPS buffer (5 mM) on $\Delta[NH_4^+]$ (*B*) and $\Delta[H^+]$ (*C*) at the yolk sac surface of larvae. Data are presented as means ± SD ($n = 10$). Different letters indicate a significant difference between pH 6, pH 7, and pH 8 (one-way ANOVA, Tukey's comparison, $P < 0.05$). *Significant difference between the NW and MOPS groups (Student's *t*-test, $P < 0.05$).

with development from 3 to 7 dpf (Fig. 3*B*). At 7 dpf, $\Delta[NH_4^+]$ was measured at the surface of gills instead of yolk sac, which was absorbed. In these stages, the NH_4^+ gradient was significantly higher in larvae exposed to 5 mM HA than larvae in NW (Fig. 3*B*).

H^+ gradients in larvae exposed to NW and 5 mm HA. The surface H^+ gradient in the yolk sac area of the larvae was also measured by SIET to compare the effects of HA on larval acid secretion. The $\Delta[H^+]$ value was positive and gradually increased with development in NW larvae (Fig. 4). However, the $\Delta[H^+]$ value of HA larvae was significantly lower than that of NW larvae, particularly in larvae exposed to HA for 5 days (the 5-pdf larvae). At that time, the $\Delta[H^+]$ of HA decreased to ~10% of control.

Effects of external pH and strong buffer on ammonium gradient. The NH_4^+ gradient in NW larvae was measured in recording media with different pH values to examine the effect of external pH on ammonium gradient. Results showed that the $\Delta[NH_4^+]$ was significantly higher in pH 6 medium than in pH 7 or pH 8 medium (Fig. 5*A*). When larvae in the medium with strong buffer (5 mM MOPS) were measured, both $\Delta[NH_4^+]$ and $\Delta[H^+]$ decreased to 64% and 54%, respectively (Fig. 5, *B* and *C*; NW contained only 300 μM MOPS).

Ammonium gradients in larvae with gene knockdown or inhibitors. To investigate the role of V-type H^+-ATPase in ammonia excretion, morpholino gene knockdown (of the *atp6v1a* gene) and bafilomycin A1 inhibition were conducted in this experiment. As shown in Fig. 6, *A* and *B*, both $\Delta[NH_4^+]$ and $\Delta[H^+]$ remarkably decreased in *atp6v1a* morphants (larvae injected with MOs). The inhibited levels of ammonium and proton gradients were both close to 70%. This inhibitory effect was also confirmed by bafilomycin A1 treatment (10 μM for 1 h), which significantly decreased both proton and ammonium gradient at larval skin (Fig. 7, *A* and *B*). In larvae injected with the *rhcg1* morpholino, $\Delta[NH_4^+]$ decreased by 36%; however, $\Delta[H^+]$ remained at the same level (Fig. 6, *C* and *D*). To verify the effect of *rhcg1* knockdown, immunostaining was done in the larvae (Fig. 8). Rhcg1-specific antibody reacted with a group of ionocytes (it has been reported to be HRCs; 17) in the yolk sac skin of wild-type (Fig. 8*A*) and control larvae (Fig. 8*D*). However, the Rhcg1 signal totally disappeared in the larvae injected with 8 ng *rhcg1* morpholino (Fig. 8*C*).

To further examine whether NHE also contributes to ammonium excretion, amiloride or EIPA (0.1, 1 mM for 10 min) was applied to the larvae. Compared with bafilomycin, the level inhibited by amiloride or EIPA was relatively low, and the levels by which acid and ammonium decreased were also similar (Fig. 7, *C* and *D*).

DISCUSSION

In the present study, we examined the mechanism of ammonia excretion in posthatched zebrafish larvae. The major findings were *1*) ammonia is mainly excreted from the yolk sac epithelium, in which HRCs excrete higher levels of acid and ammonia than do other epithelial cells; *2*) the V-type H^+-pump

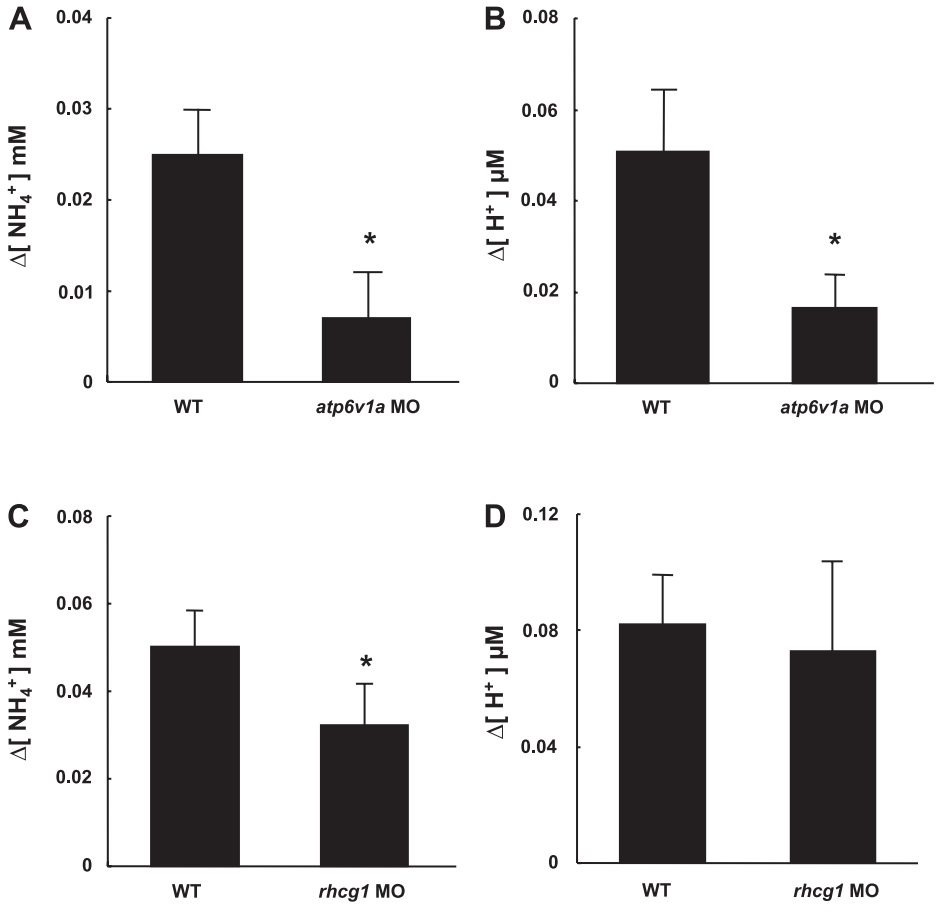

Fig. 6. $\Delta[NH_4^+]$ (*A* and *C*) and $\Delta[H^+]$ (*B* and *D*) at the yolk sac surface of wild-type (WT) larvae and morpholino (MO)-injected larvae. The morpholino against *atp6v1* or *rhcg1* was injected at the 1- to 4-cell stage of larvae, and the larvae were measured at 5 dpf. Different batches of embryos were used for the *atp6v* or *rhcg1* injection. Data are presented as means ± SD (n = 10). *Significant difference (Student's t-test, $P < 0.05$).

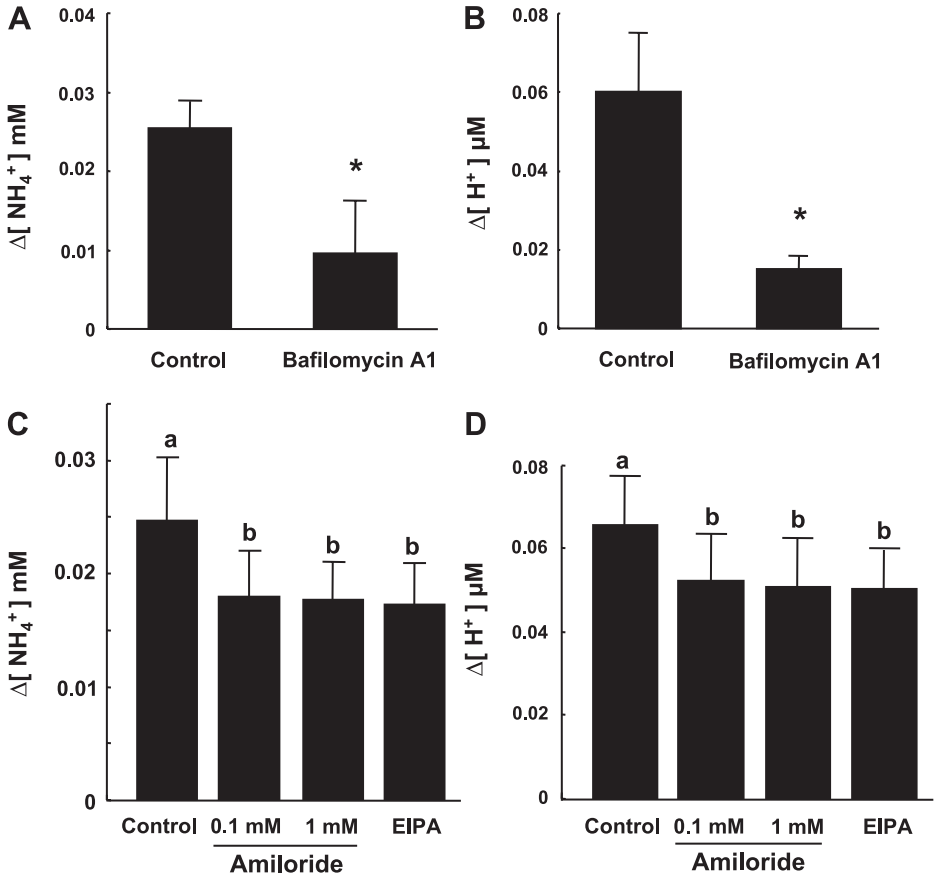

Fig. 7. Effects of bafilomycin A1 (10 μM), amiloride (0.1 mM and 1 mM), and 5-ethyl-isopropyl amiloride (EIPA; 1 mM) on $\Delta[NH_4^+]$ (*A* and *C*) and $\Delta[H^+]$ (*B* and *D*) at the yolk sac surface of zebrafish larvae. Different batches of 5-dpf larvae were used for bafilomycin A1 or amiloride treatments. Data are presented as means ± SD ($n = 10$). *Significant difference (Student's *t*-test, $P < 0.05$). Different letters indicate a significant difference (one-way ANOVA, Tukey's comparison, $P < 0.05$).

in HRCs plays a critical role in ammonia excretion by generating an external acid layer to drive transepithelial ammonia transport; and *3*) Rhcg1 in HRCs is involved in ammonia excretion.

In previous reports on fish ammonia transport, the net flux of total ammonia (including NH_3 and NH_4^+) was determined by calculating changes in total ammonia in the water during the experiment (29, 32). However, that method provides the ammonia flux from the entire animal but not specific organs or cell types. In the present study, SIET was used to measure the NH_4^+ activity and flux at specific locations on the surface of larval skin. SIET has been used to detect various ions, including H^+, K^+, Na^+, Ca^{2+}, Cl^-, etc. (2, 15, 21, 22, 23) of samples ranging from plants to animals. Unlike traditional ion-selective microelectrodes, which are used to measure intra- or extracellular ion activities, SIET detects extracellular ion activity and ion flux at specific locations. However, it should be noted that SIET measures diffusion flux of ion (calculated with Fick's law) outside of the skin or cell, instead of transepithelial (transmembrane) ion flux. Although, the extracellular ion gradient or flux is caused mainly by transmembrane ion flux, several factors may affect the measured values. In the case of H^+ probing, H^+ activity at skin surface is related to direct H^+ efflux, H^+ generated by the CO_2 hydration and loss of H^+ via titration of buffers in water and NH_3 excreted (the main point of this study). To discriminate specific source, we used inhibitors such as bafilomycin in this study to block H^+-ATPase-dependent H^+ secretion. Thus we can conclude that the measured H^+ gradient reflects transmembrane H^+ transport through H^+-ATPase to some degree.

The application of SIET to probing NH_4^+ has been reported in studies of plant root absorption (7) and mosquito NH_4^+ excretion (4). For the first time, the present study used SIET to detect cellular NH_4^+ transport in an intact vertebrate model, the zebrafish. In this study, the ammonia secreted by larval skin was presented as $\Delta[NH_4^+]$ calculated from the difference in NH_4^+ activities between the background and the location of interest. To calibrate the NH_4^+ activity and flux, a linear Nernstian regression was done using a series of known concentrations of NH_4Cl. The slope of the concentrations above 0.1 mM was fitted to a linear Nernstian slope of 58 but gradually decayed at concentrations below 0.1 mM (data not shown). However, the NH_4^+ concentration in NW was lower than 0.01 mM and was thus beyond the linear range of the calibrating line. For a practical and precise calibration, the NH_4^+ concentration in the medium for SIET measurement was raised by adding 0.1 mM NH_4Cl.

In previous studies, SIET was used to determine H^+ transport in the skin of zebrafish larvae and was shown to be a good approach for examining ion transport in a zebrafish model (9, 16). The present study further used SIET to examine ammonia transport in zebrafish and provides direct evidence for the cellular location and molecular mechanism of ammonia transport in zebrafish larvae. In a study on the air-breathing mudskipper (*Periophthalmodon schlosseri*), mitochondria-rich cells (MRCs) were suggested to be the location of branchial ammonia transport (28). In zebrafish, vH-MRCs (which refer to HRCs in our study) were also suggested to be involved in ammonia transport based on evidence of Rhcg1 in the apical membrane (17). Furthermore, pavement cells were

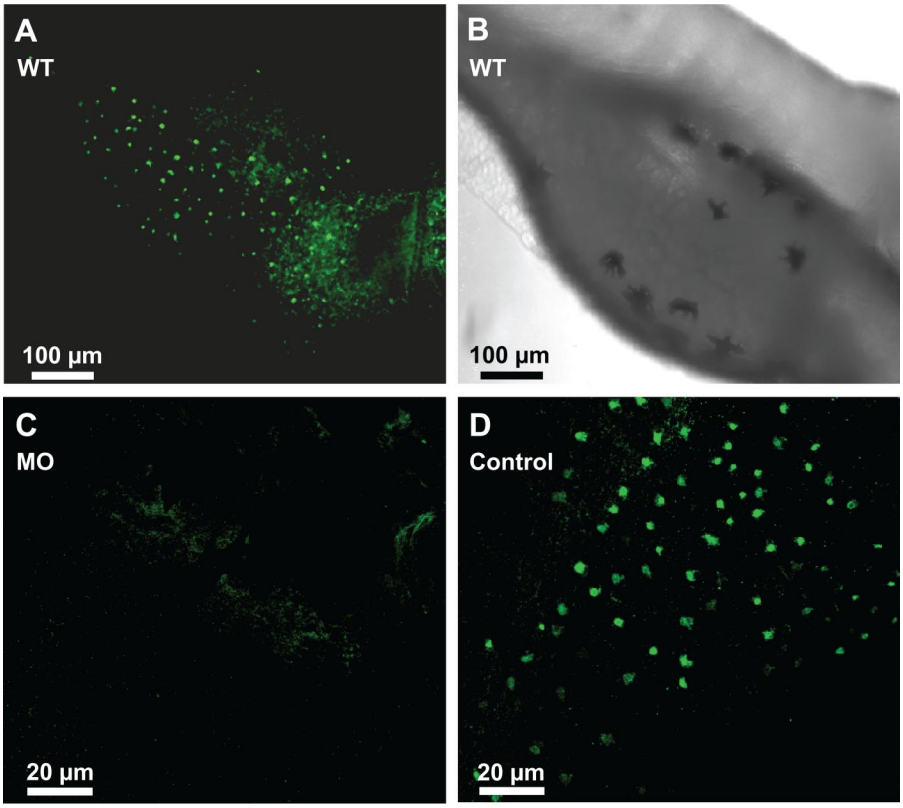

Fig. 8. Confocal laser scanning images of Rhcg1 immunostaining (green signals) in wild-type larvae (*A* and *B*), control-oligo-injected larvae (control; *D*), and Rhcg1-knockdown morphants (MO; *C*) at 5 dpf. *A* and *B* are fluorescent and transparent light images, respectively, of the same larva.

also suggested to be involved in ammonia transport of zebrafish (17), pufferfish (18), and rainbow trout (19). However, those studies provide molecular evidence for the localization of the ammonia transporter, and functional evidence on these cells has not been reported. In this study, SIET detected outward NH_4^+ fluxes of about threefold higher in HRCs than in adjacent keratinocytes or other ionocytes. This finding coincides with our previous finding that HRCs are acid-secreting cells (16) and consequently drive a significant amount of NH_3 transport by the mechanism of "acid-trapping." Although the NH_4^+ flux in HRCs is relatively high, keratinocytes should greatly contribute to overall NH_4^+ transport due to their large number and surface area.

The unstirred acid layer facilitating branchial ammonia transport (by the acid-trapping mechanism) has been proposed and may be the dominant mechanism for ammonia excretion in freshwater teleosts (25). This mechanism of skin ammonia transport was demonstrated in larval zebrafish by the present data. A high external pH (pH 8) and strong MOPS buffer (5 mM) diminished the formation of the surface acid layer (acid gradient) and consequently ammonia transport. In addition, the acid gradient at the skin surface was greatly diminished in larvae acclimated to 5 mM HA (Fig. 4). These data can be interpreted as increased NH_3 secretion from HA larvae combined (consumed) with the secreted H^+ at the skin surface thus generated a higher NH_4^+ gradient. If a larva secretes total ammonia mainly in the form of NH_4^+, we would expect to see an increase in the surface acid gradient instead of a decrease. Our data apparently do not support this point. However, we cannot completely rule out a minor portion of NH_4^+ excretion.

More importantly, we suggest that H^+-ATPase in the apical membrane of HRCs contributes >70% to skin acid secretion and the accompanying ammonia transport. Both bafilomycin inhibition and *atp6v1a* gene knockdown directly demonstrated the contribution of H^+-ATPase to NH_4^+ secretion. In contrast, CO_2 diffusion and H^+ transport by NHE contributed relatively little to acid and ammonia secretion. In gills of the mudskipper (*P. schlosseri*), NHE was suggested to play a critical role in active ammonium transport (Na^+/NH_4^+ exchange) (20); however, recent studies do not support this mechanism in freshwater fish (19). Our data show that amiloride or EIPA inhibited both H^+ and NH_4^+ secretion by ~20%, and the blocked NH_4^+ secretion was more likely due to a decrease in acid trapping than to Na^+/NH_4^+ exchange. Na^+/NH_4^+ exchange by NHE was first reported in a mammalian study in 1981 (14), in which functional assay of NHE was done with rabbit renal microvillus membrane vesicles. However, we cannot find other functional studies that convincingly demonstrate Na^+/NH_4^+ exchange by NHE with in vitro expression systems. In mammalian studies, NH_4^+ is thought to be transported by Na^+-K^+(NH_4^+)-ATPase and Na^+-K^+ (NH_4^+)-$2Cl^-$ cotransporter because of the similar property and size of K^+ and NH_4^+ (24). However, the size of H^+ and NH_4^+ is quite different. If NHE can carry NH_4^+ needs to be further studied with expression system such as *Xenopus* oocytes.

Rh glycoproteins (members of the Amt/MEP/Rh superfamily) are generally thought to function as NH_3/NH_4^+ transporters in a broad range of species (30). Recent studies suggested that Amt/MEP/Rh proteins are more like channel proteins that deprotonate NH_4^+ and then conduct NH_3 (12, 13). Four isoforms of the Rh protein (Rhag, Rhbg, Rhcg1, and Rhcg2) have been identified in the gill epithelium of zebrafish (17). Among them, Rhcg1 expression has been located in the apical membrane of HRCs in the yolk sac and gills (17). In this study, we

further conducted a loss-of-function study (*rhcg1* gene knockdown) to demonstrate the function of Rhcg1 in ammonia transport. In Rhcg1 morphants, about a 40% decrease in ammonia secretion but no significant change in acid secretion was revealed. This suggests that other Rh isoforms might also be involved in ammonia transport, and thus the effect of *rhcg1* knockdown alone was not as high as H^+-ATPase knockdown or bafilomycin treatment. Taking this evidence together, we suggest a model that H^+-ATPase in HRCs generates an extracellular H^+ gradient to drive facilitative NH_3 diffusion through Rhcg1 in HRCs and possibly through other Rh glycoproteins in keratinocytes. Further study is needed to investigate the function and regulation of other isoforms in zebrafish.

ACKNOWLEDGMENTS

We thank Dr. Shigehisa Hirose for providing antibodies against Rhcg1.

GRANTS

The authors acknowledge the National Science Council of Taiwan for grant support (NSC 96-2313-B-003-001-MY3).

REFERENCES

1. **Avella M, Bornancin M.** A new analysis of ammonia and sodium transport through the gills of fresh water rainbow trout (*Salmo gairdneri*). *J Exp Biol* 142: 155–175, 1989.
2. **Breton S, Smith PJ, Lui B, Brown D.** Acidification of the male reproductive tract by a proton pumping (H^+)-ATPase. *Nat Med* 2: 470–472, 1996.
3. **Claiborne JB, Edwards SL, Morrison-Shetlar AI.** Acid-base regulation in fishes: cellular and molecular mechanisms. *J Exp Zool* 293: 302–319, 2002.
4. **Donini A, O'Donnell MJ.** Analysis of Na^+, Cl^-, K^+, H^+ and NH_4^+ concentration gradients adjacent to the surface of anal papillae of the mosquito *Aedes aegypti*: application of self-referencing ion-selective microelectrodes. *J Exp Biol* 208: 603–610, 2005.
5. **Evans DH, Piermarini PM, Choe KP.** The multifunctional fish gill: dominant site of gas exchange, osmoregulation, acid-base regulation, and excretion of nitrogenous waste. *Physiol Rev* 85: 97–177, 2005.
6. **Faszewski EE, Kunkel JG.** Covariance of ion flux measurements allows new interpretation of *Xenopus laevis* oocyte physiology. *J Exp Zool* 290: 652–661, 2001.
7. **Henriksen GH, Bloom AJ, Spanswick RM.** Measurement of net fluxes of ammonium and nitrate at the surface of barley roots using ion-selective microelectrodes. *Plant Physiol* 93: 271–280, 1990.
8. **Hirata T, Kaneko T, Ono T, Nakazato T, Furukawa N, Hasegawa S, Wakabayashi S, Shigekawa M, Chang MH, Romero MF, Hirose S.** Mechanism of acid adaptation of a fish living in a pH 3.5 lake. *Am J Physiol Regul Integr Comp Physiol* 284: R1199–R1212, 2003.
9. **Horng JL, Lin LY, Huang CJ, Katoh F, Kaneko T, Hwang PP.** Knockdown of V-ATPase subunit A (*atp6v1a*) impairs acid secretion and ion balance in zebrafish (*Danio rerio*). *Am J Physiol Regul Integr Comp Physiol* 292: R2068–R2076, 2007.
10. **Hung CY, Tsui KN, Wilson JM, Nawata CM, Wood CM, Wright PA.** Rhesus glycoprotein gene expression in the mangrove killifish *Kryptolebias marmoratus* exposed to elevated environmental ammonia levels and air. *J Exp Biol* 210: 2419–2429, 2007.
11. **Hwang PP, Lee TH.** New insights into fish ion regulation and mitochondrion-rich cells. *Comp Biochem Physiol A Mol Integr Physiol* 148: 479–497, 2007.
12. **Javelle A, Lupo D, Ripoche P, Fulford T, Merrick M, Winkler FK.** Substrate binding, deprotonation, and selectivity at the periplasmic entrance of the *Escherichia coli* ammonia channel AmtB. *Proc Natl Acad Sci USA* 105: 5040–5045, 2008.
13. **Khademi S, O'Connell J, 3rd Remis J, Robles-Colmenares Y, Miercke LJ, Stroud RM.** Mechanism of ammonia transport by Amt/MEP/Rh: structure of AmtB at 1.35 A. *Science* 305: 1587–1594, 2004.
14. **Kinsella JL, Aronson PS.** Interaction of NH_4^+ and Li^+ with the renal microvillus membrane Na^+-H^+ exchanger. *Am J Physiol Cell Physiol* 241: C220–C226, 1981.
15. **Land SC, Sanger RH, Smith PJ.** O_2 availability modulates transmembrane Ca^{2+} flux via second-messenger pathways in anoxia-tolerant hepatocytes. *J Appl Physiol* 82: 776–783, 1997.
16. **Lin LY, Horng JL, Kunkel JG, Hwang PP.** Proton pump-rich cell secretes acid in skin of zebrafish larvae. *Am J Physiol Cell Physiol* 290: C371–C378, 2006.
17. **Nakada T, Hoshijima K, Esaki M, Nagayoshi S, Kawakami K, Hirose S.** Localization of ammonia transporter Rhcg1 in mitochondrion-rich cells of yolk sac, gill, and kidney of zebrafish and its ionic strength-dependent expression. *Am J Physiol Regul Integr Comp Physiol* 293: R1743–R1753, 2007.
18. **Nakada T, Westhoff CM, Kato A, Hirose S.** Ammonia secretion from fish gill depends on a set of Rh glycoproteins. *FASEB J* 21: 1067–1074, 2007.
19. **Nawata CM, Hung CC, Tsui TK, Wilson JM, Wright PA, Wood CM.** Ammonia excretion in rainbow trout (*Oncorhynchus mykiss*): evidence for Rh glycoprotein and H^+-ATPase involvement. *Physiol Genomics* 31: 463–474, 2007.
20. **Randall DJ, Wilson JM, Peng KW, Kok TW, Kuah SS, Chew SF, Lam TJ, Ip YK.** The mudskipper, *Periophthalmodon schlosseri*, actively transports NH_4^+ against a concentration gradient. *Am J Physiol Regul Integr Comp Physiol* 277: R1562–R1567, 1999.
21. **Shirihai O, Smith P, Hammar K, Dagan D.** Microglia generate external proton and potassium ion gradients utilizing a member of the H/K ATPase family. *Glia* 23: 339–348, 1998.
22. **Smith PJ, Sanger RH, Jaffe LF.** The vibrating Ca^{2+} electrode: a new technique for detecting plasma membrane regions of Ca^{2+} influx and efflux. *Methods Cell Biol* 40: 115–134, 1994.
23. **Smith PJ, Trimarchi J.** Noninvasive measurement of hydrogen and potassium ion flux from single cells and epithelial structures. *Am J Physiol Cell Physiol* 280: C1–C11, 2001.
24. **Weiner ID, Hamm LL.** Molecular mechanisms of renal ammonia transport. *Annu Rev Physiol* 69: 317–340, 2007.
25. **Wilkie MP.** Ammonia excretion and urea handling by fish gills: present understanding and future research challenges. *J Exp Zool* 293: 284–301, 2002.
26. **Wilkie MP.** Mechanisms of ammonia excretion across fish gills. *Comp Biochem Physiol A Mol Integr Physiol* 118: 39–50, 1997.
27. **Wilson JM, Laurent P, Tufts BL, Benos DJ, Donowitz M, Vogl AW, Randall DJ.** NaCl uptake by the branchial epithelium in freshwater teleost fish: an immunological approach to ion-transport protein localization. *J Exp Biol* 203: 2279–2296, 2000.
28. **Wilson JM, Randall DJ, Donowitz M, Vogl AW, Ip AK.** Immunolocalization of ion-transport proteins to branchial epithelium mitochondria-rich cells in the mudskipper (*Periophthalmodon schlosseri*). *J Exp Biol* 203: 2297–2310, 2000.
29. **Wilson RW, Wright PM, Munger RS, Wood CM.** Ammonia excretion in fresh water rainbow trout (*Oncorhynchus mykiss*) and the importance of gill boundary layer acidification: lack of evidence for Na^+/NH_4^+ exchange. *J Exp Biol* 191: 37–58, 1994.
30. **Winkler FK.** Amt/MEP/Rh proteins conduct ammonia. *Pflügers Arch* 451: 701–707, 2006.
31. **Wood CM.** Ammonia and urea metabolism and excretion. In: *The Physiology of Fishes*, edited by Evans DH. Boca Raton, FL: CRC, 1993, p. 379–425.
32. **Wright PA.** Nitrogen excretion and enzyme pathways for ureagenesis in fresh water tilapia (*Oreochromis niloticus*). *Physiol Zool* 66: 881–901, 1993.
33. **Wright PA, Randall DJ, Perry SF.** Fish gill water boundary layer: a site of linkage between carbon dioxide and ammonia excretion. *J Comp Physiol* 158: 627–635, 1989.
34. **Yan JJ, Chou MY, Kaneko T, Hwang PP.** Gene expression of Na^+/H^+ exchanger in zebrafish H^+-ATPase-rich cells during acclimation to low-Na^+ and acidic environments. *Am J Physiol Cell Physiol* 293: C1814–C1823, 2007.